

BlockLLM: Multi-tenant Finer-grained Serving for Large Language Models

Bodun Hu

The University of Texas at Austin

Jiamin Li

Microsoft Research

Le Xu*

The University of Texas at Austin

Myungjin Lee

Cisco Research

Akshay Jajoo

Cisco Research

Geon-Woo Kim

The University of Texas at Austin

Hong Xu

The Chinese University of Hong Kong

Aditya Akella

The University of Texas at Austin

Abstract

The increasing demand for Large Language Models (LLMs) across various applications has led to a significant shift in the design of deep learning serving systems. Deploying LLMs, particularly in multi-tenant environments, poses substantial challenges due to their high computational and memory demands. We introduce BlockLLM, a serving system that leverages component sharing among fine-tuned LLM models to provide an efficient and flexible solution for LLM workloads. BlockLLM partitions models into finer-grained blocks, enabling the reuse of model components and independent provisioning to improve computation efficiency. BlockLLM comprises an offline block zoo for storing blocks and an online system to serve requests through chains of blocks. It offers multi-fold flexibilities: (1) Adaptive assembly of blocks on-the-fly through equivalence evaluation among blocks in the zoo; (2) Per-block batch size configuration and best-effort KV cache coordination at the individual block level; (3) Speculative execution and locality-aware block placement to reduce communication costs from dynamic block resource allocation. Our evaluation shows that BlockLLM reduces memory and storage footprints and improves computational efficiency, outperforming existing serving approach in 95%ile latency and GPU utilization by 33.5% and 20.1%, respectively, with minimal impact on accuracy.

1 Introduction

The rise of Large Language Models (LLMs) marks a transformative milestone in deep learning. Their unprecedented abilities in natural language processing [36], from language translation [10] to question-answering [1] and complex reasoning [27, 49], are reshaping technological frontiers. Yet, the strength of LLMs—rooted in their vast parameter spaces—comes at the price of significant computation costs [9]. The deployment of LLMs is an arduous endeavor, often necessitating the use of hundreds or even thousands of extremely expensive computation devices like GPUs, thus imposing

great challenges on unleashing LLM’s full potential [6, 45].

Fine-tuning recently has emerged as a critical technique to efficiently adapt foundation models to handle various downstream tasks across different domains [14, 21]. Fine-tuning updates existing parameters or introduces additional parameters using domain-specific data. As LLMs become ubiquitous, the challenge of serving these fine-tuned models from a multi-tenant cluster—whether in a private cloud for first-party services or a public cloud for third-party users—has become increasingly significant.

Recent serving systems and approaches focus on model-internal optimization, such as accelerating matrix computations [2, 13], minimizing device memory fragmentation [25], and enabling parallel decoding in the auto-regressive token generation process [16, 34]. While these advancements significantly accelerate inference of individual LLMs, the challenge remains to serve multiple tenants’ fine-tuned models in a shared cluster. Each LLM requires substantial resources, and the hardware cost makes it prohibitive to liberally expand the cluster to add dedicated resources for each tenant. Thus, the question is: *how can LLM serving meet the latency goals of tenants’ fine-tuned models while also ensuring high throughput and optimal utilization cluster-wide?*

We introduce BlockLLM, an efficient and flexible serving system tailored for fine-tuned LLMs in a multi-tenant cluster. BlockLLM enables LLM model component reuse by breaking down an LLM into smaller and shareable components which we call “blocks”. The central observation forming the basis for BlockLLM is that fine-tuning offers the opportunity for *sharing*. Parameter-efficient fine-tuned models have an inherent modular architecture where parameters from specific layers are added or altered. Our observations with full-parameter fine-tuned models indicate that certain model components produce outputs with high similarity, suggesting their potential for sharing as well. Block sharing reduces both memory and storage demands. Furthermore, by reallocating memory—previously consumed by redundant parameters—towards supporting larger data batch size, BlockLLM achieves higher computation efficiency and overall throughput.

*Work done at the University of Texas at Austin.

BlockLLM consists of an offline “block zoo”—a repository of LLM blocks, and an online serving system capable of dynamically scheduling blocks to serve various applications (Figure 1). BlockLLM brings three immediate opportunities. (1) It can support adaptive serving, which enables on-the-fly assembly of blocks for each request, moving beyond the traditional static chain of blocks. (2) Each block can be individually configured, allowing for customized batch sizes and autonomous handling of queued requests. (3) BlockLLM enables dynamic resource allocation, with each block capable of independently scaling and being placed without the constraints of model-level boundaries.

Several challenges arise in realizing BlockLLM with full flexibility. First, the feasibility of adaptive serving hinges on an in-depth understanding of the equivalence among blocks. This necessitates a mechanism to establish inter-block relationship within the block zoo. Moreover, LLMs store intermediate results in KV cache [39] to avoid recalculation due to their auto-regressive nature. The independent configuration of each block leads to overlapping lifecycles of different requests, demanding stateful coordination to maintain the coherence of the KV cache across concurrent requests. Lastly, resource allocation without model-level boundaries brings extra inter-block communication, thereby imposing additional latency costs that are not easily mitigated. In BlockLLM, we propose integrated solutions for these challenges.

First, to ascertain the equivalence of blocks, we compare the output distribution of vocabulary probabilities, which serves as an indicator for functional equivalence between transformer layers. Furthermore, we investigate methods to facilitate the reuse and sharing of LLM components while minimizing any potential impact on accuracy. Inspired by the techniques of merging computer vision models [38], we design a generalizable stitching block as an intermediary to route requests among these blocks so that the chain of blocks to serve each request can be adaptively adjusted online.

Second, to manage the KV cache generated by different requests, BlockLLM employs a principled approach to request dispatching. The per-block configuration introduces complexity in handling the KV cache, particularly when requests are assigned to devices lacking the corresponding cache. This scenario necessitates either cache communication or recalculation. We analyze the trade-off between recalculation and I/O costs to determine priorities for different candidate block instances, including those specified in the chain and its equivalent blocks. We adopt a best-effort KV coordination policy, prioritizing devices that already possess the KV cache when dispatching requests.

Third, to address the inherent latency costs associated with inter-block communication, BlockLLM integrates speculative execution for identified bottleneck blocks, enabling the processing of potential request pathways in advance. We use surrogate models to predict the outputs of blocks, facilitating computation ahead of actual output. We also implement a

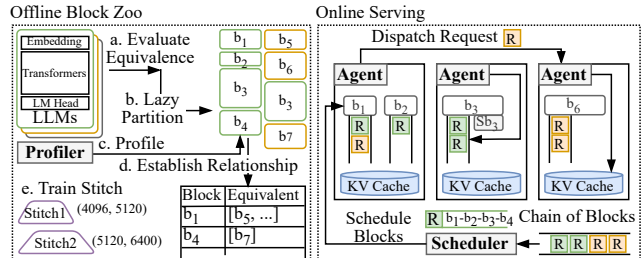


Figure 1: System architecture. b_x are blocks. ‘R’ are requests. SB_3 is the surrogates of Block b_3 .

locality-aware strategy for block placement, positioning interdependent blocks in close proximity, preferably within the same server. This approach minimizes the frequency of costly inter-server communications and leverages the high-speed intra-server connections to expedite data transfer.

We summarize our contributions as follows:

- We leverage the LLM fine-tuning characteristic and demonstrate the benefits of finer-grained LLM serving. This approach reduces memory and storage demands while optimizing computation resource utilization.
- We construct a block zoo that stores LLMs in finer granularity to enable block reuse and establishes the equivalence among these blocks to facilitate adaptive online serving.
- We build an online serving system to improve cluster throughput. It strategically coordinates the KV cache by best-effort request dispatching and minimizes communication overhead with bottleneck-pinpointing speculative execution and locality-aware placement.
- We implement and evaluate BlockLLM in a 12-A100 cluster. BlockLLM achieves comparable median latency with traditional per-model provisioning and reduces the 95%ile latency by 33.5%. The overall average throughput is elevated by 1.71x. GPU SM efficiency is improved by 20.1%.

2 Background and Motivation

2.1 Background

LLM serving. LLM-based applications have grown to become major workloads in GPU clusters, creating significant serving challenges. Large storage is required to store the model checkpoints and engines, and numerous powerful GPUs with ample memory are required to load and execute the models. [39, 44]. The auto-regressive nature of LLMs necessitates caching KV matrices to avoid redundant recalculations [40]. Each request’s KV cache grows as the generation process continues. Moreover, when models are inevitably deployed in a distributed manner, a high-capacity network is indispensable to transfer the intermediate activations. Such a burden is particularly pronounced in multi-tenant clusters, which cater to diverse LLM applications, each with its dedicated models and performance objectives.

Foundation models and fine-tuning. LLM training follows transfer learning as a guiding principle. A foundation model is initially pre-trained on a broad spectrum of general data,

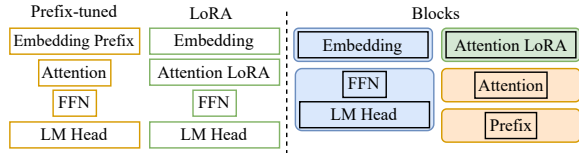


Figure 2: Example of blocks for two models fine-tuned from the same foundation. We show one Transformer layer for simplicity.

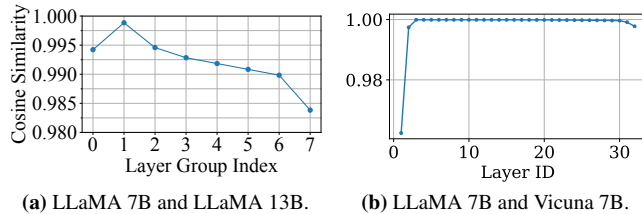


Figure 3: Output similarity between Transformer layer groups of two models, which is then customized for specific applications through fine-tuning. This process involves introducing additional parameters or modifying existing ones within the model using task-specific datasets. Fine-tuning entails updating either the entire model, known as full-parameter fine-tuning (FF) [8], or altering a small subset of additional or modified parameters, referred to as parameter-efficient fine-tuning (PE) [17, 32]. PE examples include LoRA [23], BitFit [52], Adapter [18], and Prefix-Tuning [28].

Problem statement. The wide adoption of LLM necessitates an efficient multi-tenant serving system tailored for such workloads. Beyond fulfilling latency requirements, our goal is to elevate throughput and resource utilization in a cluster where diverse LLM applications are present.

2.2 Key Idea: Finer-grained Serving

To enhance the efficiency of LLM serving systems, we advocate a finer-grained approach. Rather than treating each model as an indivisible unit, we propose BlockLLM, which partitions LLMs into smaller components provisioned independently. These components are envisioned as “blocks”. We could maintain only one copy of a block even if it is used by multiple models. The immediate benefit is the decreased demand for memory and storage.

PE models are ideal for this approach due to their inherent modular architecture. As shown in Figure 2, two models could be divided into five blocks, with blue blocks being shared components. Moreover, our analysis of FF models reveals that different blocks share highly similar outputs.

Figure 3 presents the output vocabulary distribution similarity of each Transformer layer between LLaMA 7B and LLaMA13B, as well LLaMA 7B and Vicuna 7B(FF from LLaMA), with an average similarity of 0.9927 and 0.998, respectively. This observation underpins the feasibility of reusing blocks across different FF models, thereby enhancing resource efficiency by allowing device memory to hold more critical data.

Opportunities. BlockLLM consists of an offline block zoo (§4) and an online serving system (§5). We enable block reuse

in block zoo and establish connections among blocks. In the serving phase, BlockLLM deploys the blocks onto the cluster and assembles a chain of blocks to serve each request. Each block instance is provisioned independently. Block-granularity provision brings three significant opportunities for enhancing serving flexibility.

O1: Adaptive serving. Deployment and serving can be highly adaptive. Blocks allow for dynamic assembly into a variety of model configurations. Serving a request is not constrained to a predetermined chain of blocks. Instead, it can be dynamically adjusted in real-time, based on the deployment state, to improve efficiency. The key to realizing this fully adaptive serving hinges on accurately determining whether the blocks are functionally equivalent (§4, §5.3).

O2: Per-block configuration. Each block can have its unique configuration. First, the batch size of each block could be individually configured. Intuitively, a block shared by multiple applications should have a larger batch size to efficiently handle the collective load. Second, each block maintains its own request queue and manages the request state independently, thus autonomously deciding how to process the requests. A critical consideration in this configuration is how auto-regressive models can be integrated into this paradigm, where the KV cache should be managed in a cohesive approach (§5.1).

O3: Dynamic resource allocation. BlockLLM enhances resource allocation by scaling each block independently. Blocks that are frequently accessed or computationally intensive can dynamically be allocated with more resources. It also liberates block placement from the constraints associated with monolithic model architectures. However, it does introduce a challenge in the form of increased communication costs. Effectively mitigating these costs is crucial to achieving truly versatile resource allocation within BlockLLM (§5.2, §5.3).

2.3 Comparison with Existing Work

Existing serving systems for serving LLM workloads utilize the same techniques as traditional DNN serving. Each model operates within a dedicated engine and is provisioned as a monolithic unit. An alternative approach is multi-tasking. A typical example is S-LoRA [43], which exploits memory paging to pack multiple LoRAs within one engine. Another line of optimizations focuses on the model internals—like accelerating Attention layer computations (FlashAttention [13]), managing KV cache (PagedAttention [25] in vLLM), and efficiently scheduling varying sequence lengths of requests (Orca [51]). These efforts are complementary to BlockLLM. BlockLLM tackles the inefficiency of serving LLM workloads in a multi-tenant cluster by leveraging the characteristics of LLM fine-tuning. Block-granularity provisioning improves the serving efficiency from two perspectives.

Reduced memory and storage. Models fine-tuned from the same foundation model inherit a significant number of shared parameters. We detail various fine-tuning techniques and the extent of parameter modification in Table 1 and illustrate the

Model	PE	% of Shared Params.
LLaMA 7B	LoRA (Green)	99.94
	Adapter (Purple)	92.62
	Prefix (Orange)	99.88
	LoRA	99.52
GPT-NeoX-20B	Adapter	92.52
	Prompt	99.98

Table 1: Percentage of shared parameters of different PE techniques.

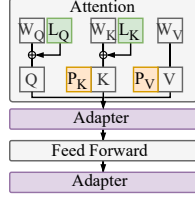


Figure 4: Architectural changes of PE.

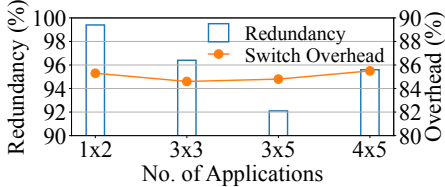


Figure 5: Redundancy and switching overhead in the existing serving system. $x \times y$ indicates we have x foundation models and y models fine-tuned from each foundation. Therefore, xy models in total.

architectural changes in Figure 4 with shared parameters depicted as gray boxes. Existing serving systems ignore this aspect, leading unfortunately to the redundant storage of identical model pieces. In Figure 5, we present the percentage of the model parameters being redundant. With more diverse applications served in a cluster, the size of redundancy is more significant. When the cluster hosts 15 LLM-based applications that are adapted from three foundation models (3rd bar), the 92.1% redundancy takes up to ~ 147 GB. In terms of memory-related operations, this redundancy becomes particularly instrumental, where models are frequently swapped in and out in response to requests from different applications. A considerable portion of the switching overhead (85.4% with 20 applications) is wastefully spent on unnecessary replacement of the same parameters. With BlockLLM, the switching overhead is reduced to at most 12.2% with 9 applications and 16.5% with 20 applications.

Improved computation efficiency. Serving each model within a standalone engine presupposes a complete execution cycle. As such, per-model provisioning prevents the sharing of computations among models, even when they contain identical components. It is inefficient in a multi-tenant cluster where many different applications are served. Table 2 shows the average latency, throughput, and GPU utilization of a small cluster of four GPUs where 40 requests from three applications are served. When using per-model provisioning, the throughput and GPU utilization are low because the batch size is small, and the devices hosting less popular applications are severely under-utilized. Alternatively, with BlockLLM, we could achieve a 34.8% higher throughput. The gain primarily stems from three aspects: (1) the reduced overhead by loading smaller model pieces, (2) higher computation efficiency due to larger batch sizes for shared blocks (O2), (3) effective scaling of popular blocks onto the idle computation resources originally reserved by less popular applications (O3). We also measure the performance improvement when the number of applications the cluster hosts grows from 3 to 12 and

No. of Apps	Per-model Provision			BlockLLM		
	Latency	Throughput	Utilization	Latency	Throughput	Utilization
3	5.4	6.6	64.4%	4.6	8.9	76.5%
6	7.6	8.2	75.1%	5.2	12.3	79.4%
9	14.4	7.2	76.6%	9.9	14.5	85.3%
12	17.6	6.9	74.4%	12.4	15.6	89.6%

Table 2: Comparison of average latency (mins/request), throughput (tokens/second), and GPU utilization (SM efficiency) when the number of applications increases. GPU utilization is measured until the last request is completed.

the number of requests grows proportionally. The throughput improvement of 12 applications is 1.91x of the throughput improvement when hosting three applications.

3 BlockLLM Design

In this section, we provide an overview of the BlockLLM’s architecture and workflow, along with a discussion of its three key design challenges.

3.1 System Overview

Architecture. Figure 1 depicts the system architecture of BlockLLM. In the preparatory offline phase, BlockLLM hosts a repository—termed “block zoo”—that houses the LLMs in blocks. It is equipped with an automated mechanism that partitions the models into blocks and ascertains the equivalence among existing blocks. Additionally, the block zoo integrates a profiler to record the performance metrics and trade-offs pertinent to each block. In the real-time online phase, BlockLLM has a scheduler that orchestrates resource allocation and placement of blocks and processes the requests. It strategically schedules blocks onto devices, denoted as “block instance”. A BlockLLM agent resides on every device in the cluster. It maintains and monitors the block instances and the associated request queues. It is responsible for handling the requests, including managing the KV cache and transferring outputs to other block instances.

Workflow. When a new request arrives, the scheduler assigns a chain of blocks based on the application it belongs to. The scheduler initially determines whether there is an available instance of the first block in the chain. If available, the request is forwarded to the target block instance. Otherwise, the scheduler either identifies a suitable alternative among the existing equivalent block instances or deploys a new block instance on an available device. Upon receipt of the request, the device’s agent directs it to the designated block instance for processing. Then, once the execution is completed, the agent is responsible for directing the request through the subsequent block in the chain. The process ends with the completion of the request signified by an EOS token, whereupon the final agent relays the output back to the scheduler, thus concluding the response cycle of the request.

3.2 Design Challenges

C1: Evaluate different-sized block equivalence. To achieve adaptive serving, establishing the equivalence between blocks

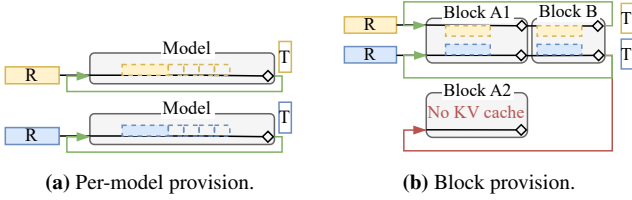


Figure 6: Illustration of coordinating KV cache when using block-granularity provisioning

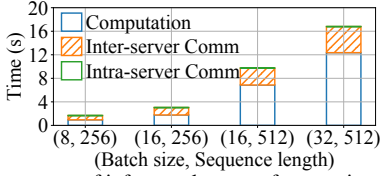


Figure 7: Components of inference latency of generating one token using LLaMA 7B in BlockLLM.

is necessary so that chains of blocks for each request can be adjusted on the fly. Block-granularity model zoo offers improved manageability compared to full models due to their significantly smaller parameter size. Nonetheless, establishing such equivalence remains a complex issue. Despite the widespread adoption of the Transformer architecture in most existing LLMs, they often vary in size-related parameters like the embedding size. While metrics such as cosine similarity or L2 norm can be employed to assess the equivalence between blocks of identical architecture, evaluating blocks of differing architectures for equivalence is far from straightforward. Furthermore, even with an understanding of their similarities, it is not feasible to directly route a request to a block that differs in embedding size.

C2: Coordinate stateful KV cache. In BlockLLM, sophisticated stateful serving is indispensable for auto-regressive LLMs. Existing serving systems operate by dedicating each model instance to process a single batch of requests until completion. This approach allows GPU devices to retain a singular, specific KV cache for the batch they are processing. However, BlockLLM introduces a more complex scenario where each block is configured independently. Each block instance may concurrently process multiple request batches over time, each generating its distinct KV cache. This interleaved processing approach, coupled with the auto-regressive nature of the tasks, implies that a request batch requiring subsequent iterations needs access to its original KV cache. However, there’s no guarantee that the same device that holds the KV cache will be available to process additional iterations of that batch. Figure 6 illustrates this challenge, showcasing how the blue request could encounter the problem of no available KV cache if dispatched to Block instance A2 under BlockLLM’s provision choice.

C3: Mitigate communication overhead. Versatile resource allocation of finer-grained blocks provides several benefits for online serving, as mentioned in §2.2. Yet BlockLLM incurs additional non-negligible communication overhead. Specifically, each time a request batch is directed to a different device, it necessitates intra-server or inter-server communi-

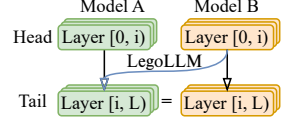


Figure 8: Routing requests when equivalence is found.

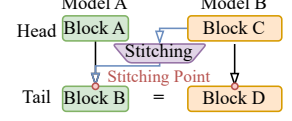


Figure 9: Stitch blocks in different embedding sizes.

cation. This communication might act as a bottleneck for the batch, directly contributing to increased latency. The communication overhead also linearly grows with the number of block instances passed by a request batch during its lifecycle. Furthermore, the volume of data transferred escalates with the use of larger batch sizes per block. Figure 7 breaks down the latency components involved in generating one new token across various request batches. Without any optimization to the communication, for a request batch of size 32 and length 512, the computation constitutes 62.9% of the total latency, whereas the inter-server communication accounts for 36.4%.

4 Block Zoo

In this section, we mainly answer three questions:

- How to evaluate equivalence among model components? (C1, §4.1)
- What are the accuracy implications of block sharing? (§4.2)
- How to partition LLMs into blocks? (§4.3)
- How to handle request routing between two equivalent blocks with different embedding sizes? (C1, §4.4)

4.1 Equivalence

PE models inherently possess equivalent components for reuse. We focus on verifying the equivalence among FF model components. Given that different models may produce outputs of varying sizes (e.g. the embedding sizes of the 7B and 13B LLaMA models are 4096 and 5120, respectively), we utilize *output vocabulary probabilities* to determine equivalence. By feeding the same data into the model, we transform the output of each Transformer layer into vocabulary probabilities and compute the cosine similarity of these probabilities as an indicator of equivalence. Figure 3 illustrates the output cosine similarity of layers partitioned from models of different sizes. Since LLaMA 7B and LLaMA 13B have different number of transformer layers, we group 3 layers from LLaMA 7B and 4 layers from LLaMA 13B into a single block for comparison. The average similarity is 0.9841 for LLaMA 7B and LLaMA 13B, and 0.998 for LLaMA 7B and Vicuna 7B.

4.2 Accuracy Implications

Block Sharing. The output equivalence between foundational models and their FF models, as well as between differently-sized foundational models, suggests potential for dividing models into sharable blocks. However, naively sharing these blocks may impact inference quality, even with high output similarity.

Figure 10a shows how block sharing affects accuracy. We

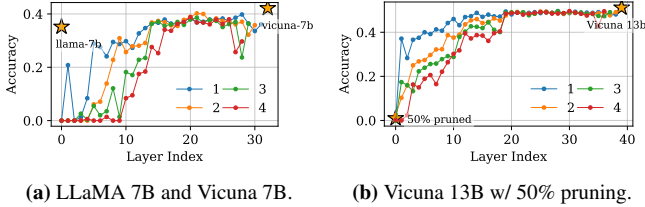


Figure 10: Block Sharing Accuracy.

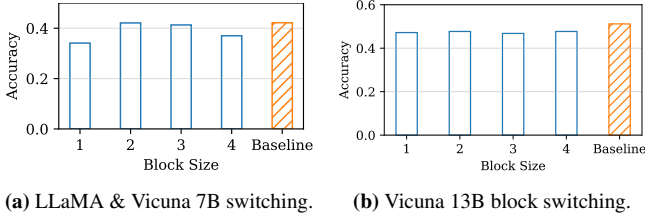


Figure 11: Block Switching Accuracy.

treated each decoding layer as a single block and tested various numbers of shared blocks at different layer positions. For instance, with four blocks, we used layers 0-3 of LLaMA 7B and layers 4-31 of Vicuna 7B, then layers 1-4 of LLaMA 7B and layers 0, 5-31 of Vicuna 7B, and so on. The figure shows significant accuracy impact when sharing occurs at initial layers, but minimal impact at middle and end layers.

This trend is consistent even with different block configurations. Figure 10b shows a similar pattern when applying 50% parameter pruning to blocks. Unlike the previous experiment, we only use blocks from Vicuna 13B, and applied 50% parameter pruning to selected blocks. The results indicate that pruning near the middle and end blocks has minimal accuracy impact, while initial blocks are less affected. Therefore, block sharing should be prioritized for middle or end components before initial ones. This phenomenon has also been observed in previous studies [7, 11, 24, 33], likely due to redundancy in later layers.

Block Switching. The design of BlockLLM allows a request to be processed by an arbitrary block at any point, which may result in a single request frequently switching between blocks and potentially affecting inference quality. Figure 11a shows the impact of frequent block switching on accuracy. We selected layer 16 as the starting point for block switching due to stable accuracy and treated x subsequent layers as a single block. For each block after layer 16, we continuously switch blocks between two models. For instance, if $x = 2$, a request will use layers 17-18 from Vicuna 7B, then switch to layers 19-20 of LLaMA 7B, then switch back to layers 21-22 of Vicuna 7B, and so on. We applied a similar switching strategy to 50% pruned Vicuna 7B blocks. Figures 11a and 11b show that frequent block switching near the end has minimal impact on accuracy. In practice, the switching does not occur so frequently due to excessive communication overhead.

4.3 Model Partitioning

With the evaluated equivalence and accuracy, BlockLLM incorporates an automated mechanism that breaks down LLMs

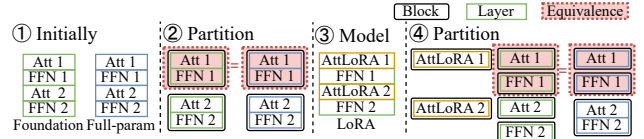


Figure 12: An example of BlockLLM's lazy partitioning.

into blocks. Each block then becomes an independent engine during serving.

Principles of constructing block zoo. BlockLLM follows two guiding principles: (1) avoid over-partitioning, (2) the preservation of architectural integrity. In this way, BlockLLM can reuse the blocks with minimal additional effort.

The rationale for reducing redundancy is to prevent unnecessary duplication. If one model component has no variant, it is meaningless to over-partition it into excessively small blocks. Such miniature partitioning is inefficient both in terms of computational power within each block and due to the increased overhead from data transfer between blocks.

The second principle directs BlockLLM to partition the model only at clear architectural boundaries. Based on PE and FF techniques we have adopted [8, 17, 32, 46], BlockLLM sets the following network components as the finest-grained network components that can compose a block: *attention*, *ffn*, *embedding*, *lm_head*. This approach ensures that the output of one block seamlessly serves as the input to another, facilitating a streamlined chain of blocks for each request. BlockLLM avoids intricate arithmetic operations between blocks, simplifying the challenge of assembling them during the serving process. An illustrative example is the application of LoRA to two Linear operations within an Attention layer. Isolating LoRA as a separate block would lead to the partitioning of the Attention layer into five blocks, requiring BlockLLM to sum up the outputs of the LoRA block and the foundation Attention block. Therefore, in BlockLLM, each Attention with LoRA layer should be a separate block.

Lazy partitioning. BlockLLM employs a lazy partitioning strategy for all fine-tuned models utilizing a foundation model, slicing models as needed without preset restrictions on the size or architecture of the blocks. For PE models, it is partitioned into two blocks, the foundation model and its PE adapter.

As for FF models, after BlockLLM evaluates equivalence between model components (§4.1), we perform lazy partitioning. As shown in Figure 12, for an FF model adapted from the foundation model (①), BlockLLM sets a threshold T and group *all connected network components* (e.g., transformer layer 1 from the fine-tuned model and the foundation) that have equivalence exceeding T into a block (②). This action results in 4 blocks, with two blocks being considered equivalent. When a newly added PE model (e.g., LoRA) arrives (③), BlockLLM (1) preserve its PE adapters (e.g., AttLoRA1, AttLoRA2), (2) find all existing blocks that share parameters (e.g., FFN1, FFN2) with the new model and (3) attempts to partition the existing blocks to enable block reuse. LoRA here

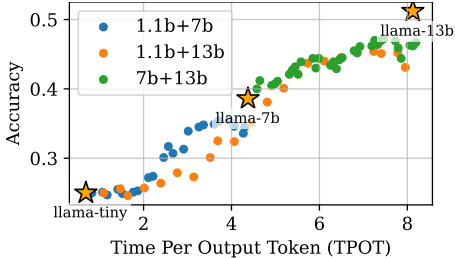


Figure 13: Accuracy & TPOT after applying a stitching layer to LLaMA (1.1B, 7B, 13B)

Stitching Block	GPU hours	LM Head Cosine Similarity
(2048, 4096)	2.01	0.9634
(4096, 5120)	4.33	0.9732
(5120, 4096)	4.84	0.9683
(4096, 8192)	6.32	0.9798
(5120, 8192)	5.85	0.9612

Table 3: Costs of training a stitching block in different sizes on A100 GPUs and output similarity with the large model.

has a different Attention layer. Therefore, we *further* partition the foundation model into four blocks so that they share the FFN layers in separately-provisioned blocks (④). This action results in 9 blocks with two chain-of-blocks being equivalent.

It is important to note that BlockLLM uses blocks as logical basic units of resource provisioning, and the granularity of blocks does not necessarily introduce overhead during serving time: BlockLLM considers overhead of pipelining blocks at fine-granularity and could choose to allocate consecutive chain of blocks in a single agent. The engine executes these blocks as a single network sub-component.

4.4 Stitching Block

While requests can be directly routed between blocks with the same embedding sizes, this does not apply to blocks of different embedding sizes. When two blocks of different embedding sizes are considered equivalent, such as Blocks B and D illustrated in Figure 9, routing requests originally intended for Block B to D presents a unique challenge.

Stitching blocks. We propose to use a stitching block, a concept that has been recently explored [38]. We follow the principle of fine-tuning LLMs to obtain a stitching block. However, training a unique stitching block for each potential block pair is impractical. Thus, our objective is to design a *generalizable* stitching block. When multiple equivalences are identified between blocks originating from the same two foundation models, requests can be seamlessly redirected at any stitching point using the stitching block.

We use a Linear layer to serve as the stitching block. This stitching block is trained while keeping the parameters of other blocks static. This approach is inspired by [38]. To generalize the stitching block, we encode the positional information of the stitching point as an extra dimension. The position value is the sum of the positions of the head block and the tail block in their original foundation model. During training, the stitching block is initially placed at a shallow

layer and progressively moved to deeper ones. This approach follows the idea of reusing layers in [29, 50]. Table 3 shows the training costs and the performance of the stitched model compared with the large model. Figure 13 shows the accuracy and latency when applying stitching block between different decoding layers in LLaMA 1.1B, 7B, and 13B.

The underlying hypothesis of our approach is rooted in the Transformer-based architecture of LLMs: the output embedding from any Transformer layer can be interpreted as natural language. This characteristic presents the opportunity to engineer a stitching block with the unique capability of translating the output embedding from one dimension to another. This strategy allows the integration of varied block sizes.

5 Online Serving

We now present BlockLLM’s online serving system. We first explain how BlockLLM deals with stateful KV cache (C2, §5.1). Then, we discuss BlockLLM’s two strategies to mitigate the impact of communication overhead (C3, §5.2, §5.3).

5.1 KV Cache Coordination

Memory bandwidth-bound KV cache. Efficient stateful coordination of the KV cache is crucial for auto-regressive LLMs in BlockLLM, as memory bandwidth constraints on the KV cache have been identified as a significant bottleneck in numerous studies. Existing systems process one batch of requests at a time, weighing the trade-off between recalculating the KV matrices and caching them in device memory. This trade-off reaches a point—determined by factors such as device type, model architecture, and request sequence length—where caching becomes more efficient than recalculation. However, as request sequences lengthen, memory bandwidth constraints become a performance-bounding factor when loading the KV cache [25].

I/O and recalculation cost. As aforementioned in §3.2, BlockLLM’s design complicates the problem. The assumption that requests are consistently processed by the same block instances no longer holds, making I/O costs for transferring KV caches between instances unavoidable.

To migrate the KV cache from device d_i to d_j , we optimize the process by overlapping KV cache recomputation with copying, thereby minimizing migration time. Given the fully known context, we employ chunked prefilling for efficient recomputation. For sequences to be migrated, denoted as $S = s_i^n$, we begin by recomputing the KV cache from the start of sequence s_1 while simultaneously copying the cache starting from the end of sequence s_n . The process concludes when recomputation encounters a KV cache page that has already been copied, indicating the completion of migration.

This approach is chosen for two key reasons. First, each token’s KV cache depends on the KV caches of all preceding tokens. Recomputing the KV cache from the beginning of a sequence ensures the accuracy of the entire cache. In contrast, copying can take place independently, without relying on pre-

ceding caches. Second, ongoing requests on the target device may introduce latency during recomputation. By employing chunked prefill, we improve GPU utilization and mitigate the impact of KV cache recomputation on other tasks.

Proactive KV Cache Migration. As BlockLLM may redirect requests to blocks lacking the necessary KV caches, this can introduce additional migration latency. While this overhead cannot be completely eliminated, it can be mitigated by proactively migrating KV caches in advance, thereby removing it from the critical path.

To ensure that migration does not introduce latency, it is essential to predict whether the KV cache will be used before the migration completes. The feasibility of predicting KV cache usage has been demonstrated in [4]. We adopt the method proposed in [4] to estimate the interception time: $T_{INT} = t_{now} - t_{call}$, where t_{now} is the current time updated for each iteration, and t_{call} is the time when the last interception was initiated.

Memory Efficiency. Modern LLM inference serving systems support paged attention [25], a technique that partitions the KV cache into smaller pages. This approach eliminates the need to store the entire KV cache in contiguous memory and allows for the sharing of KV cache pages across multiple requests, thereby enhancing memory efficiency. However, dynamically routing requests to blocks that lack the required KV cache can result in the creation of new KV cache pages. Since each device maintains its own dedicated KV cache page table, generating the same KV cache page on a different device leads to the duplication of KV pages. This duplication, which otherwise would only require a single KV page with an incremented reference counter, undermines the advantages of memory sharing.

To prevent memory waste, we prioritize migrating pages referenced by fewer requests before those referenced by more. We denote all KV pages as $C = \{c_1, c_2, \dots, c_n\}$, where each c_i represents the underlying consecutive KV pages of request s_i , and n is the total number of requests tracked by the system. We use $ref(c_i)$ to calculate the total number of pages referenced by more than one request in sequence s_i . For KV cache pages $c_i \in C$, we have $ref(c_i) \leq ref(c_{i+1})$. If $ref(c_i) = ref(c_{i+1})$, then $resumeTime(c_i) \leq resumeTime(c_{i+1})$, where $resumeTime(c_i)$ is the estimated time the pages c_i will be reused by the intercepted request s_i .

Prioritize KV cache owner. Transferring KV caches to a new block instance can introduce latency, impacting request processing times. This latency is subject to network bandwidth and varying network conditions. Although recalculating the KV cache can sometimes be more efficient than direct copying, it may still disrupt ongoing requests on the target device. Therefore, we prioritize block instances that already possess the required KV cache before redirecting requests to a new device. This approach follows the principle of best-effort coordination. When candidate block instances have the same status (e.g., queuing time), BlockLLM’s agent prioritizes dis-

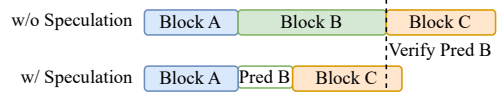


Figure 14: Speculative execution of Block B.

Block	Pruned Percentage	Cosine Similarity	Computation Speedup
5th Attention	49.71%	0.7	37.43×
5th FFN	49.83%	0.77	1.71×
5th Transformer	49.79%	0.94	22.91×
5th–7th Transformers	49.79%	0.84	18.55×

Table 4: Performance of blocks’ surrogates in terms of prediction similarity and computation time. Blocks are pruned from LLaMA 7B based on the structured pruning technique described in [30].

patching the request to the block instance that holds the associated KV cache. In §5.3, we provide a detailed discussion on how BlockLLM’s agent selects the appropriate block instance.

5.2 Speculative Execution

Request transfer overhead negatively impacts overall throughput in two significant ways. First, it directly and inevitably increases inference latency due to its inherent blocking nature: each subsequent block’s operation depends on receiving output from the preceding block, creating a strong dependency. Second, it depletes network resources, as each redirection of a request to a different server involves network transfer. In BlockLLM, we address the first issue with speculative execution and the second with block scheduling and placement.

Reduce latency via ahead-of-time prediction. Considerable efforts have been dedicated to enhancing P2P network transfers [41, 56], and such optimizations could be leveraged in BlockLLM to diminish inference latency. However, our approach seeks to offset any latency increases by accelerating the inference pipeline itself. Drawing from the design in the operating system, we exploit speculative execution to expedite the inference process. Instead of awaiting actual outputs from a preceding block, it predicts the outcome, allowing subsequent blocks to proceed based on these predictions. Should the predictions align with the actual results, this speculation can lead to reduced latency. As illustrated in Figure 14, when Block B adopts speculative execution using Pred B, the inference latency is shorter if it is verified to be a correct prediction.

The challenge of a successful speculation lies in both the time and the accuracy of the prediction. If the prediction takes a longer time than the actual computation, the benefits of speculation are nullified. If the accuracy of predictions is low, reliance on the actual output becomes inevitable to ensure computational correctness, rendering the speculative efforts both redundant and a potential drain on resources.

Block surrogates. We leverage insights from existing work and empirical studies, coupled with our block zoo, to construct high-fidelity surrogates for the blocks. The surrogates are used for prediction. First, we consider pruned models. One typical pruning technique is sparse models. While sparsity typically results in a reduction of computation FLOPs, it does not always correspond to a commensurate decrease

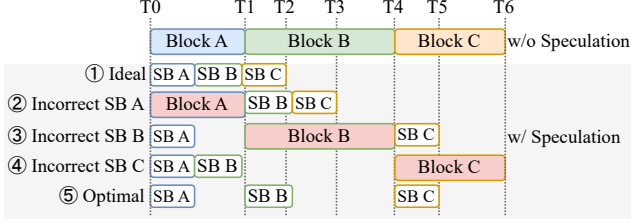


Figure 15: Possible scenarios when speculative execution is consecutively applied to all blocks.

in computation time. Hence, our focus is on pruning techniques that meaningfully cut down computation time. We implement a strategy inspired by existing literature [30] to construct surrogates for our blocks. In particular, we perform structured pruning by selectively removing sub-structure that generates less critical impact towards the model output and then add fine-tuned LoRA for performance recovery after the pruning process. Table 4 shows the output similarity and computation time of four blocks and their surrogates. Second, we exploit equivalent blocks with different computation costs. For instance, a block partitioned from a 7B LLaMA model can serve as an effective surrogate for a block from a 30B LLaMA model, which is adopted by [34].

Bottleneck-pinpointing speculation. Naively applying speculative execution to blocks does not guarantee latency improvement, as it requires verifying the predicted results. In Figure 15, consider an inference pipeline composed of three blocks where speculative execution is applied to each. Ideally, if all speculations are destined to be correct, the inference latency is expected to be reduced from T6 to T2 (①). However, consecutive prediction verification can diminish these gains, especially when erroneous predictions happen at the latter part of the chain. For instance, if a prediction error arises at Block C (last block in the chain) (④), the latency reduction would only be 0, compared to a reduction of T6-T3 if the error occurred earlier at Block A (②). Therefore, the optimal inference (⑤) one could achieve is T5 instead of T2, because each speculative block needs to wait for the completion of the bigger verification block. In the worst case, where all three speculations are incorrect, there would be no latency reduction at all. Practically, due to the concurrent execution of blocks and their surrogates, this could even result in additional slowdowns.

To avoid such outcomes, we follow two rules when implementing speculation. First, we avoid enabling speculation on consecutive blocks to minimize accumulated errors and wasted resources. Second, speculation is not applied at the last block in the chain because the final output, once relayed back to BlockLLM’s scheduler, is not correctable. Thus, during serving, we selectively apply speculation to the top- k bottleneck blocks—those characterized by their computation intensity or frequent use. The performance of speculative inference is evaluated in §7.3.

5.3 Request and Block Scheduling

Adaptive serving. BlockLLM’s scheduler and agents perform adaptive serving when dispatching the request to a suitable block instance. With the help of block zoo, the candidate block instances for each request include the block that is explicitly listed in the chain and its equivalent blocks.

BlockLLM’s request scheduling strategy prioritizes block instances that hold a request’s KV cache, provided the device memory can accommodate the request data. If the device memory cannot hold the data, the strategy estimates the latency of each candidate instance and schedules the request to the instance with the lowest latency increase. When a block does not have a request’s KV cache, the latency estimation for a candidate block instance on device c is as follows:

$$\begin{aligned}
 Latency_{d_c} &= T_{queue} + T_{compute} + T_{transfer} + T_{load}, \\
 T_{queue} &= \sum_{i=1}^n Comp(req_i), \\
 T_{compute} &= Comp(req), \\
 T_{transfer} &= \begin{cases} T_{transfer}^{w/kv} & \text{agents dispatch,} \\ \frac{D_{req}}{B_{net}(s, d_c)} & \text{scheduler dispatches,} \end{cases} \\
 T_{load} &= \begin{cases} \max(T_{swap} - T_{transfer}, 0) & \text{idle device,} \\ T_{swap} & \text{loading overhead,} \end{cases} \\
 T_{swap} &= \frac{D_{b'}}{B_{mem}(d_c)} + \frac{D_b}{B_{net}(d_c)}.
 \end{aligned}$$

We incorporate four key factors: queuing (T_{queue}), computation ($T_{compute}$), transfer ($T_{transfer}$), and the overhead associated with block switching (T_{load}). T_{queue} accounts for the duration required to process all n queuing request batches. $T_{transfer}$ is subject to who initiates the dispatch: if done by the scheduler s , the request batch is at the start of the chain and no KV cache is involved. Otherwise, agent dispatching includes the costs of migrating the request and its KV cache (discussed in §5.1). Here, D_{req} is the size of the request token, and $B_{net}(s, d_j)$ denotes the network bandwidth between two devices. T_{load} depends on the current status of the device. If the device is busy, this loading overhead only includes T_{swap} , the time to move out the existing block b' and load the new block b . If idle, the block’s loading can be overlapped with other operations. Therefore, the loading overhead is $T_{swap} - T_{transfer}$. In T_{swap} , $B_{mem}(d_c)$ is the device memory bandwidth of candidate d_c ; $D_{b'}$ is the size of an existing block b' . For simplicity, we keep block inside device memory and leave block swapping between other storage options for future work.

Block resource allocation. BlockLLM’s scheduler determines the resource allocation of blocks, similar to a traditional serving system. We discuss BlockLLM’s strategy for enabling independent per-block scaling and speculative execution. For scaling, we follow a straightforward policy centered on the

queue length of the block instance. If the queue length exceeds $t\%$ of the maximum queue length (i.e. saturating all the device memory), we scale onto more devices starting from the most heavy-loaded block instances. If the block instance to be scaled possesses requests’ KV cache, we balance the load by moving the state as well. As for speculative execution, BlockLLM actively applies to the top- k time-consuming block instances to accelerate the inference pipeline. BlockLLM deploys surrogates using a dedicated stream on the same device where the blocks to be speculated are situated.

Locality-aware block placement. BlockLLM’s second effort to mitigate the transfer overhead is the strategic placement of blocks, aiming to reduce the reliance on network resources. During placement, BlockLLM prioritizes locality—ensuring that blocks with frequent direct inter-dependencies are close to each other. Ideally, these blocks are placed on the same server. Such an arrangement leverages the full potential of high-capacity intra-server connections, such as NVLink interconnects, for the transfer of requests and KV cache, rather than resorting to the constrained inter-server links.

In BlockLLM, the locality is quantified by monitoring historical traffic, specifically by a counter recording the frequency of being directly inter-dependent between two blocks. Block pairs with a higher locality value are placed within the same server. Furthermore, BlockLLM’s scheduler dynamically adapts to evolving traffic patterns; should the observed locality change, block instances are migrated as necessary to align with the new pattern. The benefit of locality-aware placement is discussed in §7.3.

6 Design Details

We have implemented a prototype of BlockLLM on top of vLLM. It is compatible with HuggingFace models. We use NCCL for data transfer among servers.

Profiling. To support the online serving system, BlockLLM profiles blocks by measuring computation time under different batch sizes, including surrogates and multiplexing performance. It also measures communication time between devices using NCCL primitives and the overhead of loading the block engine from disk to host and device memory.

Batching. Computation efficiency improves with larger batch sizes, but enforcing a fixed large batch size complicates request reorganization. Therefore, BlockLLM loosely encourages batching within each block instance. Upon receiving a new batch, BlockLLM’s agent queues it and attempts to pack it with neighboring requests, ensuring the combined batch does not exceed the upper batch size limit. If no requests are queued, the agent processes the batch directly. Requests reaching EOS are removed from the batch and sent to the scheduler.

Request dispatching. BlockLLM’s agents use a FIFO+priority queue, prioritizing requests that have left KV cache memory. Each block instance maintains a countdown clock for auto-regressive requests, prioritizing

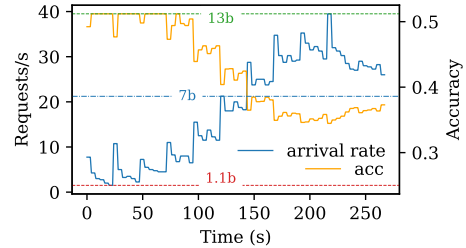


Figure 16: Accuracy and request arrival rate changes.

their return. The scheduler and agents dispatch requests differently: agents determine candidate blocks and pack them, broadcasting requests to available agents. The scheduler maintains a live record of block placements, simplifying dispatching.

7 Evaluation

We evaluate BlockLLM using testbed experiments. We seek to answer three main questions:

- What impact does BlockLLM has on accuracy? (§7.2)
- Does BlockLLM improve the overall throughput and resource utilization compared to existing solutions? (§7.2)
- For online serving, how much latency reduction is contributed by BlockLLM’s key designs? (§7.3)

7.1 Setup

Cluster. Our cluster has four servers, each of which is equipped with A100 GPUs with 80GB memory. Two servers have two GPUs, and the other two have four GPUs. The servers are interconnected with 100 Gbps links.

LLM Models. We use two foundation models in different sizes: 6B Chat-GLM [53], 7B LLaMA, and 13B LLaMA [48]. We consider fine-tuning techniques, including FF (Vicuna [8]) and PE (Prefix-Tuning, Adapter, BitFit, and LoRA). We have 20 fined-tuned LLM models, each representing an application.

Workload. We generate both production and synthetic workload traces (Figure 17) to evaluate BlockLLM’s performance. For synthetic traces, we use uniform distribution to determine the mean rate for each application. The mean rate serves as the weight to calculate the number of requests per application, creating varying popularity among applications. The arrival time of each request in one application is generated using a Poisson process with the given mean rate. The trace spans 20 minutes and includes 400 requests, following a generation approach similar to [43]. For production traces, we use timing information from a Twitter trace collected over a month-long period [3]. We set the minimum QPS to 1 and maximum QPS to 45. Previous work has shown this trace accurately reflects realistic inference workloads, exhibiting diurnal patterns and unexpected spikes [54].

Baselines. We benchmark BlockLLM with two baselines.

- Per-Model provisioning (PM): Each LLM is deployed independently. Models are scaled along with traffic demand.
- Parameter Sharing (PS): We merge PE LLMs from the same foundation and deploy them as a complete unit, similar to

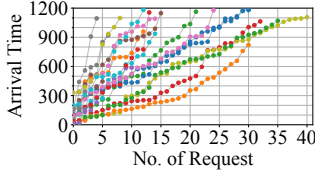


Figure 17: 20-min workload.

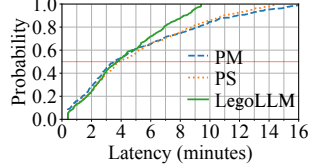


Figure 18: Latency CDF.

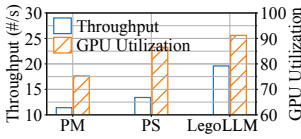


Figure 19: Throughput and GPU utilization.

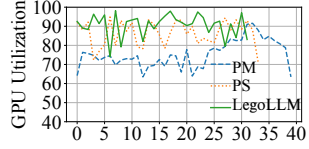


Figure 20: GPU utilization change over time.

S-LoRA [43]. Since we support various fine-tuned applications, we use branching to differentiate each application. **Metrics.** We evaluate BlockLLM with several metrics, including latency of serving one request, throughput (number of tokens per second), communication costs (percentage of time spent on data transferring), GPU utilization (SM efficiency), device memory consumption, and end-to-end accuracy.

BlockLLM’s configuration. In this evaluation, we apply speculative execution to the top 10% bottlenecked block instances sorted by the time of completing their request queues. BlockLLM’s scheduler checks redundant KV cache every one minute. We set 0.95 as the cosine similarity threshold for determining whether BlockLLM’s surrogate prediction is accurate and 0.98 as the threshold for determining equivalence. The maximum sequence length allowed is 1024. BlockLLM trains the stitching block with the MMLU [19].

7.2 Overall Performance

We first evaluate the overall performance of BlockLLM. The default number of applications is 20.

Accuracy. We use the production Twitter traces to study how accuracy reacts to changing request arrival rate. Figure 16 illustrates the variation in accuracy over time under different arrival rates. The models evaluated include LLaMA 1.1B, 7B, and 13B. Incoming requests prioritize the highest-accuracy blocks (13B) unless resources are unavailable. The average accuracy achieved is 42.1%, which is 3.5% higher than the closest option (7B). Higher request arrival rates cause BlockLLM to redirect traffic to faster but less accurate blocks (1.1B) more frequently, resulting in a gradual decline in accuracy.

Latency and throughput. Figure 18 depicts the CDF of the latency of completing a request in BlockLLM. BlockLLM’s median latency is 3.34 min, comparable with PM (3.39 min) and PS (3.87 min). The reduction of 95%ile latency is more significant, 33.5% and 23.4% compared with PM and PS. The throughput of BlockLLM is 1.71x of PM and 1.46x of PS (Figure 19). By decomposing models into more granular blocks, BlockLLM enhances the efficiency of processing larger batch sizes. This approach significantly reduces tail latency, especially under high request rates. Though PS can serve various applications within one model, the cost of one

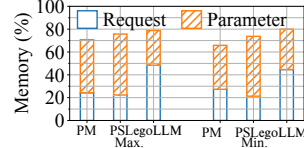


Figure 21: Memory usage of parameters and request-related data.

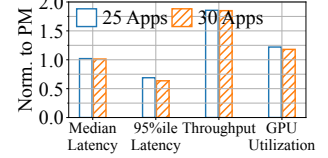


Figure 22: Performance changes when the number of applications grows.

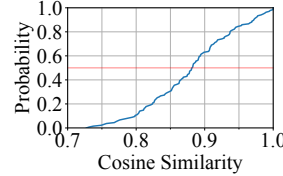


Figure 23: Cosine similarity of output vocabulary using adaptive serving and predetermined block chains.

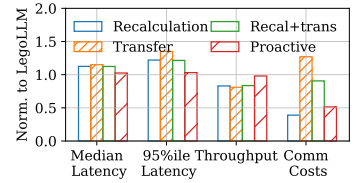


Figure 24: Ablation study of KV cache coordination strategy.

inference process grows due to branching.

GPU utilization. We also measure overall GPU utilization indicated by SM efficiency and memory consumption in the cluster. We monitor the end-to-end serving process, and the average GPU utilization is improved by 20.1% and 4.8% compared with PM and PS. Figure 20 depicts the GPU utilization change over the serving process. With the help of adaptive serving, BlockLLM efficiently dispatches requests under the existing deployment status to avoid frequent model loading and unloading. We measure the memory consumption of model parameters and request-related matrices (including input, intermediate activations, output, and KV cache). In the best case, BlockLLM takes 16.1% less space on model parameters and 24.1% more space on request-related matrices, indicating more data are being processed.

Number of applications. We increase the number of applications from 10 to 30 with the same approach in §7.1. When the number of applications grows to 30, and resources become increasingly constrained, BlockLLM’s performance gain is more prominent, achieving a 37.4% reduction in 95%ile latency and a 1.85x improvement in overall throughput (Figure 22). BlockLLM exploits block reuse to serve more applications under the same resource constraints and its flexibility brings efficiency in request serving.

7.3 Effectiveness of BlockLLM’s Design

We then evaluate the effectiveness of BlockLLM’s key designs via an ablation study.

Adaptive serving. We summarize the statistics of adaptive serving in BlockLLM. When all the requests allow adaptive servings, 136 out of 400 requests are served with adaptive chains of blocks. We compare the output vocabulary probabilities of these requests to the ones without adaptive serving and depict the cosine similarity CDF in Figure 23. The average similarity is 0.88. We disable adaptive serving in BlockLLM and the 95%ile latency and throughput are degraded by 15.6%

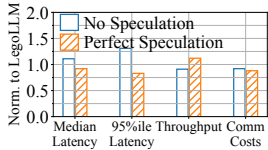


Figure 25: Ablation study of speculation: no speculation and perfect speculation.

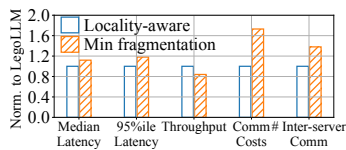


Figure 26: BlockLLM compared with fragmentation-minimized placement.

and 23.7%, respectively.

Best-effort KV cache coordination. BlockLLM performs best-effort dispatching by prioritizing the device with its KV cache memory. We consider two other solutions to verify if BlockLLM’s strategy is efficient: (1) All the KV cache are obtained using recalculation. (2) We always route the request back to the least busy device and let the KV cache owner transfer the cache to the instance. Figure 24 shows the median and 95%ile latency, throughput, and communication costs normalized to BlockLLM. The 95%ile latency is increased by 1.23x using recalculation and by 1.36x using least-busy-device routing. The communication costs are reduced significantly to 0.36 of BlockLLM when using recalculation and increased to 1.28x when using least-busy-device routing.

Speculative execution. We evaluate the effectiveness of BlockLLM’s speculative execution via two approaches in Figure 25. First, we disable speculative execution and compare BlockLLM’s performance change. The median and 95%ile latency inflates by 11.3% and 31.6%, compared with BlockLLM with speculative execution. In this evaluation, speculative execution has been performed 231 times, 192 out of which have made predictions accurate enough to avoid correction. Second, we replace our surrogates with pseudo surrogates, where we assume their predictions are always accurate with an ideal 1/50 computation time of the speculated block. The ideal 95%ile latency and throughput are 87.3% and 112.8% of BlockLLM with real surrogates. This shows that our surrogates are both efficient and accurate.

Locality-aware block placement. We compare the communication costs between BlockLLM’s locality-aware placement and the widely adopted fragmentation-minimized (frag-min) placement. Figure 26 shows the average performance change of using the frag-min placement. The median and 95%ile latency is increased by 12.6% and 18.2%. The communication costs of one request sum up all the transfer costs, therefore presenting a significant inflation of 73.4%. The locality-aware placement has reduced 72.3% inter-server communications compared with the frag-min placement strategy.

8 Discussion

Stitching models in different sizes. The concept of model concatenation, particularly across varying sizes, has been investigated in prior research with notable efforts in Convolutional Neural Networks and Transformers [15, 38]. In BlockLLM, we introduce a simple technique to validate the potential of stitching blocks of disparate sizes, ensuring that

such integration is only executed between blocks verified to be equivalent. However, it has limitations; it typically requires retraining and the maintenance of the original layer order. To overcome these limitations, a more advanced strategy is imperative based on a deeper comprehension of the models’ underlying representations and functionalities.

Other opportunities. BlockLLM’s design brings other practical benefits. (1) Partial updates. Parameter updates can be applied in block-granularity as well. With actor model [20, 31], updates can be performed concurrently with the serving process without interruption. Given the update frequency difference between the foundation and fine-tuning models, partial updates could effectively upgrade the system whenever necessary. (2) Early-exit [47] is a promising approach to reducing computation costs. However, batching limits its potential because the requests requiring the deepest computation always bottleneck the process. BlockLLM’s design choices naturally fit with early-exit, where requests can jump out of the batch at any block, which is similar to DVABatch [12], which tries to enable early-exit via multi-entry multi-exit batching.

9 Related Work

System for LLM models. Model-internal optimization including FasterTransformer [2], PagedAttention [25], FlashAttention [13] and FlexGen [44] are complimentary to BlockLLM’s contributions. Orca [51] introduces iteration-level scheduling to handle the sequence length difference among multiple requests. SpotServe [35] enables LLM serving on preemptible instances with minimized communication costs and stateful recovery. PetS [55] unifies four representative PE techniques, allowing simultaneous execution of requests from different applications, similar to Parameter Sharing in §7. [5, 22, 42] investigate accuracy-scaling to adapt to fluctuating workloads.

Auto-regressive. The inherent auto-regressive nature of LLMs limits their efficiency, making parallel decoding a key research focus. SpecInfer [34] and [26] address the issue with speculative execution, using smaller models to predict multiple tokens in advance. [16, 37] improve this by eliminating surrogate models, using the existing model with a few look-ahead tokens. These strategies generate multiple drafts to speed up token production. On the other hand, BlockLLM applies speculative execution at the block-level in a selective manner, optimizing the generation process at the individual token level.

10 Conclusion

We present BlockLLM, a multi-tenant finer-grained serving system tailored for LLM workloads. In BlockLLM, we show the effectiveness of improving throughput by allowing model component reuse with blocks. We enable adaptive serving, effectively coordinate multiple requests’ KV cache, and mitigate the communication costs to improve serving efficiency. Experiments show the efficiency of BlockLLM. We plan to

extend BlockLLM to support more models and evaluate it on larger-scale clusters.

References

- [1] ChatGPT: Optimizing Language Models for Dialogue. <https://openai.com/blog/chatgpt/>.
- [2] FasterTransformer. <https://github.com/NVIDIA/FasterTransformer>.
- [3] Twitter traces. <https://archive.org/details/archiveteam-twitter-stream-2018-04>, 2018.
- [4] Reyna Abhyankar, Zijian He, Vikranth Srivatsa, Hao Zhang, and Yiyang Zhang. Infercept: Efficient intercept support for augmented large language model inference. In *Forty-first International Conference on Machine Learning*, 2024.
- [5] Sohaib Ahmad, Hui Guan, Brian D. Friedman, Thomas Williams, Ramesh K. Sitaraman, and Thomas Woo. Proteus: A high-throughput inference-serving system with accuracy scaling. In *Proceedings of the 29th ACM International Conference on Architectural Support for Programming Languages and Operating Systems, Volume 1*, ASPLOS '24, page 318–334, New York, NY, USA, 2024. Association for Computing Machinery.
- [6] Reza Yazdani Aminabadi, Samyam Rajbhandari, Ammar Ahmad Awan, Cheng Li, Du Li, Elton Zheng, Olatunji Ruwase, Shaden Smith, Minjia Zhang, Jeff Rasley, et al. DeepSpeed-inference: enabling efficient inference of transformer models at unprecedented scale. In *SC22: International Conference for High Performance Computing, Networking, Storage and Analysis*, pages 1–15. IEEE, 2022.
- [7] Yuchen Bian, Jiayi Huang, Xingyu Cai, Jiahong Yuan, and Kenneth Church. On attention redundancy: A comprehensive study. In Kristina Toutanova, Anna Rumshisky, Luke Zettlemoyer, Dilek Hakkani-Tur, Iz Beltagy, Steven Bethard, Ryan Cotterell, Tanmoy Chakraborty, and Yichao Zhou, editors, *Proceedings of the 2021 Conference of the North American Chapter of the Association for Computational Linguistics: Human Language Technologies*, pages 930–945, Online, June 2021. Association for Computational Linguistics.
- [8] Wei-Lin Chiang, Zhuohan Li, Zi Lin, Ying Sheng, Zhanghao Wu, Hao Zhang, Lianmin Zheng, Siyuan Zhuang, Yonghao Zhuang, Joseph E. Gonzalez, Ion Stoica, and Eric P. Xing. Vicuna: An open-source chatbot impressing gpt-4 with 90%* chatgpt quality, March 2023.
- [9] Aakanksha Chowdhery, Sharan Narang, Jacob Devlin, Maarten Bosma, Gaurav Mishra, Adam Roberts, Paul Barham, Hyung Won Chung, Charles Sutton, Sebastian Gehrmann, et al. Palm: Scaling language modeling with pathways. *arXiv preprint arXiv:2204.02311*, 2022.
- [10] Alexis Conneau and Guillaume Lample. Cross-lingual language model pretraining. *Advances in neural information processing systems*, 32, 2019.
- [11] Luciano Del Corro, Allie Del Giorno, Sahaj Agarwal, Bin Yu, Ahmed Awadallah, and Subhabrata Mukherjee. Skipdecode: Autoregressive skip decoding with batching and caching for efficient llm inference, 2023.
- [12] Weihao Cui, Han Zhao, Quan Chen, Hao Wei, Zirui Li, Deze Zeng, Chao Li, and Minyi Guo. {DVABatch}: Diversity-aware {Multi-Entry}{Multi-Exit} batching for efficient processing of {DNN} services on {GPUs}. In *2022 USENIX Annual Technical Conference (USENIX ATC 22)*, pages 183–198, 2022.
- [13] Tri Dao. Flashattention-2: Faster attention with better parallelism and work partitioning. *arXiv preprint arXiv:2307.08691*, 2023.
- [14] Ning Ding, Yujia Qin, Guang Yang, Fuchao Wei, Zonghan Yang, Yusheng Su, Shengding Hu, Yulin Chen, Chi-Min Chan, Weize Chen, et al. Parameter-efficient fine-tuning of large-scale pre-trained language models. *Nature Machine Intelligence*, 5(3):220–235, 2023.
- [15] Xingli Fang, Richard M Bradford, and Jung-Eun Kim. Cooperative learning for cost-adaptive inference. In *Workshop on Advancing Neural Network Training: Computational Efficiency, Scalability, and Resource Optimization (WANT@ NeurIPS 2023)*, 2023.
- [16] Yichao Fu, Peter Bailis, Ion Stoica, and Hao Zhang. Breaking the sequential dependency of llm inference using lookahead decoding, November 2023.
- [17] Junxian He, Chunting Zhou, Xuezhe Ma, Taylor Berg-Kirkpatrick, and Graham Neubig. Towards a unified view of parameter-efficient transfer learning. In *International Conference on Learning Representations*, 2021.
- [18] Ruidan He, Linlin Liu, Hai Ye, Qingyu Tan, Bosheng Ding, Liying Cheng, Jia-Wei Low, Lidong Bing, and Luo Si. On the effectiveness of adapter-based tuning for pretrained language model adaptation. *arXiv preprint arXiv:2106.03164*, 2021.
- [19] Dan Hendrycks, Collin Burns, Steven Basart, Andy Zou, Mantas Mazeika, Dawn Song, and Jacob Steinhardt. Measuring massive multitask language understanding. *arXiv preprint arXiv:2009.03300*, 2020.
- [20] Carl Hewitt. Actor model of computation: scalable robust information systems. *arXiv preprint arXiv:1008.1459*, 2010.

- [21] Neil Houlsby, Andrei Giurgiu, Stanislaw Jastrzebski, Bruna Morroni, Quentin De Laroussilhe, Andrea Gesmundo, Mona Attariyan, and Sylvain Gelly. Parameter-efficient transfer learning for nlp. In *International Conference on Machine Learning*, pages 2790–2799. PMLR, 2019.
- [22] Bodun Hu, Le Xu, Jeongyoon Moon, Neeraja J. Yadwadkar, and Aditya Akella. Mosel: Inference serving using dynamic modality selection, 2023.
- [23] Edward J Hu, Yelong Shen, Phillip Wallis, Zeyuan Allen-Zhu, Yuanzhi Li, Shean Wang, Lu Wang, and Weizhu Chen. Lora: Low-rank adaptation of large language models. *arXiv preprint arXiv:2106.09685*, 2021.
- [24] Ajay Jaiswal, Bodun Hu, Lu Yin, Yeonju Ro, Shiwei Liu, Tianlong Chen, and Aditya Akella. Ffn-skipllm: A hidden gem for autoregressive decoding with adaptive feed forward skipping, 2024.
- [25] Woosuk Kwon, Zhuohan Li, Siyuan Zhuang, Ying Sheng, Lianmin Zheng, Cody Hao Yu, Joseph Gonzalez, Hao Zhang, and Ion Stoica. Efficient memory management for large language model serving with page-dattention. In *Proceedings of the 29th Symposium on Operating Systems Principles*, pages 611–626, 2023.
- [26] Yaniv Leviathan, Matan Kalman, and Yossi Matias. Fast inference from transformers via speculative decoding. In *International Conference on Machine Learning*, pages 19274–19286. PMLR, 2023.
- [27] Aitor Lewkowycz, Anders Andreassen, David Dohan, Ethan Dyer, Henryk Michalewski, Vinay Ramasesh, Ambrose Slone, Cem Anil, Imanol Schlag, Theo Gutman-Solo, et al. Solving quantitative reasoning problems with language models. *Advances in Neural Information Processing Systems*, 35:3843–3857, 2022.
- [28] Xiang Lisa Li and Percy Liang. Prefix-tuning: Optimizing continuous prompts for generation. *arXiv preprint arXiv:2101.00190*, 2021.
- [29] Sangkug Lym, Armand Behroozi, Wei Wen, Ge Li, Yongkee Kwon, and Mattan Erez. Mini-batch serialization: Cnn training with inter-layer data reuse. *Proceedings of Machine Learning and Systems*, 1:264–275, 2019.
- [30] Xinyin Ma, Gongfan Fang, and Xinchao Wang. Llm-pruner: On the structural pruning of large language models. In *Advances in Neural Information Processing Systems*, 2023.
- [31] Luo Mai, Kai Zeng, Rahul Potharaju, Le Xu, Steve Suh, Shivaram Venkataraman, Paolo Costa, Terry Kim, Saravanan Muthukrishnan, Vamsi Kuppa, et al. Chi: A scalable and programmable control plane for distributed stream processing systems. *Proceedings of the VLDB Endowment*, 11(10):1303–1316, 2018.
- [32] Sourab Mangrulkar, Sylvain Gugger, Lysandre Debut, Younes Belkada, Sayak Paul, and Benjamin Bossan. Peft: State-of-the-art parameter-efficient fine-tuning methods. <https://github.com/huggingface/peft>, 2022.
- [33] Xin Men, Mingyu Xu, Qingyu Zhang, Bingning Wang, Hongyu Lin, Yaojie Lu, Xianpei Han, and Weipeng Chen. Shortgpt: Layers in large language models are more redundant than you expect, 2024.
- [34] Xupeng Miao, Gabriele Oliaro, Zhihao Zhang, Xinhao Cheng, Zeyu Wang, Rae Ying Yee Wong, Zhuoming Chen, Daiyaan Arfeen, Reyna Abhyankar, and Zhihao Jia. Specinfer: Accelerating generative llm serving with speculative inference and token tree verification. *arXiv preprint arXiv:2305.09781*, 2023.
- [35] Xupeng Miao, Chunan Shi, Jiangfei Duan, Xiaoli Xi, Dahua Lin, Bin Cui, and Zhihao Jia. Spotserve: Serving generative large language models on preemptible instances. *arXiv preprint arXiv:2311.15566*, 2023.
- [36] Bonan Min, Hayley Ross, Elicor Sulem, Amir Pouran Ben Veyseh, Thien Huu Nguyen, Oscar Sainz, Eneko Agirre, Ilana Heintz, and Dan Roth. Recent advances in natural language processing via large pre-trained language models: A survey. *ACM Computing Surveys*, 56(2):1–40, 2023.
- [37] Giovanni Monea, Armand Joulin, and Edouard Grave. Pass: Parallel speculative sampling. *arXiv preprint arXiv:2311.13581*, 2023.
- [38] Zizheng Pan, Jianfei Cai, and Bohan Zhuang. Stitchable neural networks. In *Proceedings of the IEEE/CVF Conference on Computer Vision and Pattern Recognition*, pages 16102–16112, 2023.
- [39] Reiner Pope, Sholto Douglas, Aakanksha Chowdhery, Jacob Devlin, James Bradbury, Jonathan Heek, Kefan Xiao, Shivani Agrawal, and Jeff Dean. Efficiently scaling transformer inference. *Proceedings of Machine Learning and Systems*, 5, 2023.
- [40] Alec Radford, Jeffrey Wu, Rewon Child, David Luan, Dario Amodei, Ilya Sutskever, et al. Language models are unsupervised multitask learners. *OpenAI blog*, 1(8):9, 2019.
- [41] Sudarsanan Rajasekaran, Manya Ghobadi, Gautam Kumar, and Aditya Akella. Congestion control in machine learning clusters. In *Proceedings of the 21st ACM Workshop on Hot Topics in Networks*, pages 235–242, 2022.

- [42] Francisco Romero, Qian Li, Neeraja J. Yadwadkar, and Christos Kozyrakis. INFaaS: Automated model-less inference serving. In *2021 USENIX Annual Technical Conference (USENIX ATC 21)*, pages 397–411. USENIX Association, July 2021.
- [43] Ying Sheng, Shiyi Cao, Dacheng Li, Coleman Hooper, Nicholas Lee, Shuo Yang, Christopher Chou, Banghua Zhu, Lianmin Zheng, Kurt Keutzer, et al. S-lora: Serving thousands of concurrent lora adapters. *arXiv preprint arXiv:2311.03285*, 2023.
- [44] Ying Sheng, Lianmin Zheng, Binhang Yuan, Zhuohan Li, Max Ryabinin, Beidi Chen, Percy Liang, Christopher Ré, Ion Stoica, and Ce Zhang. Flexgen: high-throughput generative inference of large language models with a single gpu. In *International Conference on Machine Learning*, pages 31094–31116. PMLR, 2023.
- [45] Mohammad Shoeybi, Mostofa Patwary, Raul Puri, Patrick LeGresley, Jared Casper, and Bryan Catanzaro. Megatron-lm: Training multi-billion parameter language models using model parallelism. *arXiv preprint arXiv:1909.08053*, 2019.
- [46] Rohan Taori, Ishaan Gulrajani, Tianyi Zhang, Yann Dubois, Xuechen Li, Carlos Guestrin, Percy Liang, and Tatsunori B. Hashimoto. Stanford alpaca: An instruction-following llama model. https://github.com/tatsu-lab/stanford_alpaca, 2023.
- [47] Surat Teerapittayanon, Bradley McDanel, and Hsiang-Tsung Kung. Branchynet: Fast inference via early exiting from deep neural networks. In *2016 23rd international conference on pattern recognition (ICPR)*, pages 2464–2469. IEEE, 2016.
- [48] Hugo Touvron, Thibaut Lavril, Gautier Izacard, Xavier Martinet, Marie-Anne Lachaux, Timothée Lacroix, Baptiste Rozière, Naman Goyal, Eric Hambro, Faisal Azhar, et al. Llama: Open and efficient foundation language models. *arXiv preprint arXiv:2302.13971*, 2023.
- [49] Jason Wei, Xuezhi Wang, Dale Schuurmans, Maarten Bosma, Fei Xia, Ed Chi, Quoc V Le, Denny Zhou, et al. Chain-of-thought prompting elicits reasoning in large language models. *Advances in Neural Information Processing Systems*, 35:24824–24837, 2022.
- [50] Yang Yang, De-Chuan Zhan, Ying Fan, Yuan Jiang, and Zhi-Hua Zhou. Deep learning for fixed model reuse. In *Proceedings of the AAAI Conference on Artificial Intelligence*, volume 31, 2017.
- [51] Gyeong-In Yu, Joo Seong Jeong, Geon-Woo Kim, Soojeong Kim, and Byung-Gon Chun. Orca: A distributed serving system for {Transformer-Based} generative models. In *16th USENIX Symposium on Operating Systems Design and Implementation (OSDI 22)*, pages 521–538, 2022.
- [52] Elad Ben Zaken, Shauli Ravfogel, and Yoav Goldberg. Bitfit: Simple parameter-efficient fine-tuning for transformer-based masked language-models. *arXiv preprint arXiv:2106.10199*, 2021.
- [53] Aohan Zeng, Xiao Liu, Zhengxiao Du, Zihan Wang, Hanyu Lai, Ming Ding, Zhuoyi Yang, Yifan Xu, Wendi Zheng, Xiao Xia, Weng Lam Tam, Zixuan Ma, Yufei Xue, Jidong Zhai, Wenguang Chen, Zhiyuan Liu, Peng Zhang, Yuxiao Dong, and Jie Tang. GLM-130b: An open bilingual pre-trained model. In *The Eleventh International Conference on Learning Representations (ICLR)*, 2023.
- [54] Chengliang Zhang, Minchen Yu, Wei Wang, and Feng Yan. Mark: Exploiting cloud services for Cost-Effective, SLO-Aware machine learning inference serving. In *2019 USENIX Annual Technical Conference (USENIX ATC 19)*, pages 1049–1062, Renton, WA, July 2019. USENIX Association.
- [55] Zhe Zhou, Xuechao Wei, Jiejing Zhang, and Guangyu Sun. PetS: A unified framework for Parameter-Efficient transformers serving. In *2022 USENIX Annual Technical Conference (USENIX ATC 22)*, pages 489–504, Carlsbad, CA, July 2022. USENIX Association.
- [56] Yibo Zhu, Haggai Eran, Daniel Firestone, Chuanxiong Guo, Marina Lipshteyn, Yehonatan Liron, Jitendra Padhye, Shachar Raindel, Mohamad Haj Yahia, and Ming Zhang. Congestion control for large-scale rdma deployments. *ACM SIGCOMM Computer Communication Review*, 45(4):523–536, 2015.